Available online at www.sciencedirect.com
SCIENCE DIRECT®
Journal of Solid State Chemistry 178 (2005) 2873–2879
JOURNAL OF SOLID STATE CHEMISTRY
www.elsevier.com/locate/jssc

Effect of Niobium doping on structural, thermal, sintering and electrical properties of $Bi_4V_{1.8}Cu_{0.2}O_{10.7}$

M. Alga[a], A. Ammar[a], B. Tanouti[a], A. Outzourhit[b], F. Mauvy[c,*], R. Decourt[c]

[a]*Centre d'Excellence de Recherche sur les Matériaux, Université Cadi Ayyad, Faculté des Sciences Semlalia, Marrakech, Maroc*
[b]*Laboratoire de Physique du Solide et des Couches Minces, Département de physique, Faculté des Sciences Semlalia, Marrakech, Maroc*
[c]*Institut de Chimie de la Matière Condensée de Bordeaux, Av. Dr A.Schweitzer, 33608, Pessac, France*

Received 25 March 2005; received in revised form 18 May 2005; accepted 13 June 2005

Abstract

Doping $Bi_4V_{1.8}Cu_{0.2}O_{10.7}$ with niobium has led to the formation of the $Bi_4V_{1.8}Cu_{0.2-x}Nb_xO_{10.7+3x/2}$ solid solution. X-ray diffraction and thermal analysis have shown that only the compound with $x = 0.05$ presents a tetragonal symmetry with a γ' polymorph while the other compositions are of β polymorph. The influence of sintering temperature on the microstructure of the samples was investigated by the scanning electron microscopy (SEM). The ceramics sintered at temperatures higher than 820 °C present micro-craks. The evolution of the electrical conductivity with temperature and the degree of substitution has been investigated by impedance spectroscopy. Among all compositions studied the sample with $x = 0.05$ presents the highest value of the conductivity.

Keywords: Aurivillius phases; Ionic conductors; BIMEVOX materials; Solid electrolyte

1. Introduction

Since the discovery of the ferroelectricity in the Aurivillius compounds, after three years of the preparation of the first phase of the family [1], several laboratories throughout the world have been interested in these new materials [2–7]. Therefore, more than 70 new products have been synthesized and their ferroelectric properties studied. The structure of these phases consist of alternating $(Bi_2O_2)^{2+}$ layers and $(A_{n-1}B_nO_{3n+1})^{2-}$ groupments with perovskite-like sheets, built from edge-sharing octahedral. Generally, they obey the following formula: $(Bi_2O_2)(A_{n-1}B_nO_{3n+1})$ where A is a mono, di or trivalent ion and B a cation with average size and could be iron, aluminium, tungsten, etc., and n represents the number of perovskite-slabs.

The Aurivillius phases with higher n values are electrical insulators, and no publication dealing with the oxygen ionic conductivity has been reported in the literature, besides that published by Kendall et al. in 1994 [8] and which has been disputed thereafter by Snedden et al. [9]. This feature is due to the intolerance of this kind of Aurivillius phases to oxide ion vacancies. By contrast, the $Bi_4V_2O_{11}$, compound with $n = 1$ and which was first reported in 1986 by Russian researchers [10], presents 0.5 vacancies in the anionic sublattice, leading to an important ionic conductivity at a relatively low temperature [11]. This phase exists in three polymorphs α, β and γ. The α-$Bi_4V_2O_{11}$ (orthorhombic) exists between the room temperature and 450 °C. The β variety (orthorhombic) is stable between 450 and 580 °C; and beyond this temperature we find the γ polymorph (tetragonal). The γ-$Bi_4V_2O_{11}$ is characterized by a large disorder of oxygen atoms of the $(VO_{3.5})^{2-}$ blocks which is responsible for the high ionic conductivity (0.2 S cm^{-1} at 600 °C [11]) (Table 1).

*Corresponding author. Fax: +33 5 40 00 83 73.
E-mail address: mauvy@icmcb-bordeaux.cnrs.fr (F. Mauvy).

0022-4596/$ - see front matter © 2005 Elsevier Inc. All rights reserved.
doi:10.1016/j.jssc.2005.06.030

Table 1
Values of sintered density, relative density and grain size at different sintering temperatures

x	Sintering temperature (°C)	Density[a] (g/cm^3) (from mass and sizes)	Relative density (%)	Grain size (μm)
0.05	780	6.43±0.05	82.4	6–10
	800	6.55±0.05	84	8–12
	830	6.45±0.05	82.7	16–22
0.10	780	6.47±0.05	82.8	5–8
	800	6.57±0.05	84.2	10–12
	830	6.41±0.05	82.3	15–20
0.15	780	6.44±0.05	82.6	7–10
	800	6.51±0.05	83.7	10–12
	830	6.46±0.05	82.9	15–21

[a]The listed values of density represent average values of density measured on two pellets.

Abraham et al. have succeeded in 1990 to stabilize the γ polymorph by doping $Bi_4V_2O_{11}$ with copper leading to a new series of solid solutions known under the acronym BIMEVOX and formulated $Bi_4V_{2-x}M_xO_{11-\delta}$ [12]. Since then intensive studies of other BIMEVOX materials have been carried out [13–26] and have demonstrated their technological interest as separator of oxygen from air [27] and as cathode in primary lithium batteries: For instance $Bi_4V_2O_{11}$ react with 28 lithium ions per formula and develop a high theoretical specific energy of 840 Wh kg^{-1} [28]. Also, it has been established that the best conductivities is always obtained when 10% of V^{5+} in the native phase, $Bi_4V_2O_{11}$, has been substituted by 10% of the metal independently of its oxidation state and its nature [29]. Some other works have focused on $Bi_4V_{1.8}M_{0,1}M'_{0,1}O_{11-\delta}$ solid solutions (M is a divalent element and M' is tetra or pentavalent cations) with the aim of an enhancement of the ionic conductivity by some "synergic effect" [30–32]. So, we have recently reported detailed study of materials obtained by double substitution of V^{5+} by copper and cobalt in the limit of 10% [32] and we have found that the electrical performances have been improved. However, it is worthwhile to point out that the effect of the double substitution on the electrical properties is diverse. If Vannier et al. have not observed any improvement in the oxide anion conductivity in the case of materials with M and $M' = Cu^{2+}$, Ni^{2+} and Zn^{2+} [30], Paydar, in contrast, has recently reported an increase of the ionic conductivity of the compound with $M = Cu^{2+}$ and $M' = Ti^{4+}$ [31].

Since no particular rule explaining the diverse in the results has been pointed out, we have undertaken the study of doubly substitution of vanadium in $Bi_4V_2O_{11}$ by mixture of two metals $M = Cu^{2+}$ and $M' = Nb^{5+}$ in the limit of 10%. We have chosen the niobium owing to the important conductivity of $Bi_4V_{1.8}Nb_{0.2}O_{11}$ at relatively moderate temperature $\approx 2.5 \times 10^{-2}\,\Omega^{-1}\,cm^{-1}$ at 550 °C, in spite of its orthorhombic symmetry [33].

Hence, the purpose of this paper is to investigate the effect of such double substitution on the physical properties of the prepared ceramics.

2. Experimental

Different compositions of $Bi_4V_{1.8}Cu_{0.2-x}Nb_xO_{11+3x/2}$ solid solutions, $x = 0.05$, 0.1 and 0.15 have been prepared by conventional solid-state reaction between the corresponding reagent grade oxides. The weighted powders were thoroughly homogenized and grinded in agate mortar, then baked in a furnace at 800 °C for 24 h and slowly cooled to room temperature. Several thermal treatments with intermediate regrinding were necessary to obtain pure microcrystalline powders. The powder samples were characterized by X-ray diffraction using an XPERT MPD Philips diffractometer with Cu$K\alpha$ radiation. The patterns were recorded between 10° and 60° (2θ), with a step of 0.02° (2θ) and counting time of 4 s per step.

Thermogravimetric analysis (TGA) and differential thermal analysis (DTA) experiments were carried out between 25 and 800 °C on all the samples using an AT 1500 analyzer at a heating rate of 10 °C min^{-1}. About 20 mg of sample was used for each run.

For the shrinkage studies the powder obtained were milled for 2 h with zirconia ball (20 mm diameter) to reduce the mean particle size. After milling, the powder was sieved with 100 and 25 μm sieves. The fraction below 25 μm was put in the form of cylindrical pellets, about 6 mm diameters and 2 mm thickness, by soft uniaxial hand pressing (0.5 tonne/cm^2). The pellets were sintered, in air, according to the following conditions:

- pellets were introduced into the furnace, the temperature of which has been first stabilized at the sintering temperature T_s;
- the samples were held at T_s for 30 min and quenched from that temperature.

For scanning electron microscopy observations, the faces of the sintered pellets were polished with SiC paper (240–4000 grit) and cleaned with acetone. Microstructural observations were performed on polished samples using a Jeol 5500 scanning electron microscope. Grain boundaries were revealed by thermal etching for 20 min at 50 °C below the sintering temperature. The polished surfaces were coated with a carbon thin film.

The sample conductivity was determined by ac impedance spectroscopy in the frequency range 0.01–1 MHz using a Solartron SI 1260 Impedance Gain Phase Analyser. The amplitude of the ac signal applied across the sample was 50 mV. Measurements were

performed on sintered pellets at 800 °C for 10 h (relative density ≈84%). Pt electrodes were deposited on both flat surfaces of the pellets. For each data point, the measurements were made under dry air from 120 to 680 °C, after a 30 min stabilisation time. The experimental impedance spectra were simulated by equivalent circuits composed of resistances and constant phase elements (CPE). Values of circuit parameters were determined by non-linear least-square fitting using the Zview software.

3. Result and discussion

3.1. X-ray characterization and thermal analysis

The X-ray diffraction patterns, at room temperature, of different compositions, with $x = 0.05$, 0.10 and 0.15 are given in Fig. 1. The solid solution is fully formed for all the compositions. However, the only sample that present a tetragonal symmetry is with $x = 0.05$. The X-ray diffraction patterns of the materials with $x = 0.10$ and 0.15 are characterized by the presence of a narrow doublet at about 32°, ascribed to (020) and (200) reflections which are characteristic of the β-$Bi_4V_2O_{11}$ form. Therefore, these rates of substitution do not stabilize the tetragonal form. This result is different from what we have observed for $Bi_4V_{1.8}Cu_{0.2-x}Co_xO_{11+3x/2}$ solid solution, in which all the compositions present a tetragonal structure, but it is in agreement with a beta form obtained for neighbouring compound free of copper ($Bi_4V_{1.8}Nb_{0.2}O_{11}$) [33]. The amount of vacancies created in the anionic sublattice seems to plays an important role in stabilizing the high temperature form of $Bi_4V_2O_{11}$.

The variations of the unit cell parameters and the volume as a function of the niobium content are reported in Fig. 2. When the fraction of Nb^{5+} increases, a progressive increase of these parameters is observed. This trend is different from what it is expected if we take into account only the larger effective ionic radius of Cu^{2+} (0.74 Å) compared with Nb^{5+} (0.64 Å) [34]. However, it could be explained by the predominance of the decrease of oxygen vacancies in the Nb substituted phases. Actually, there is competition between oxygen vacancies that tend to increase the unit cell volume when x increases and the difference of the

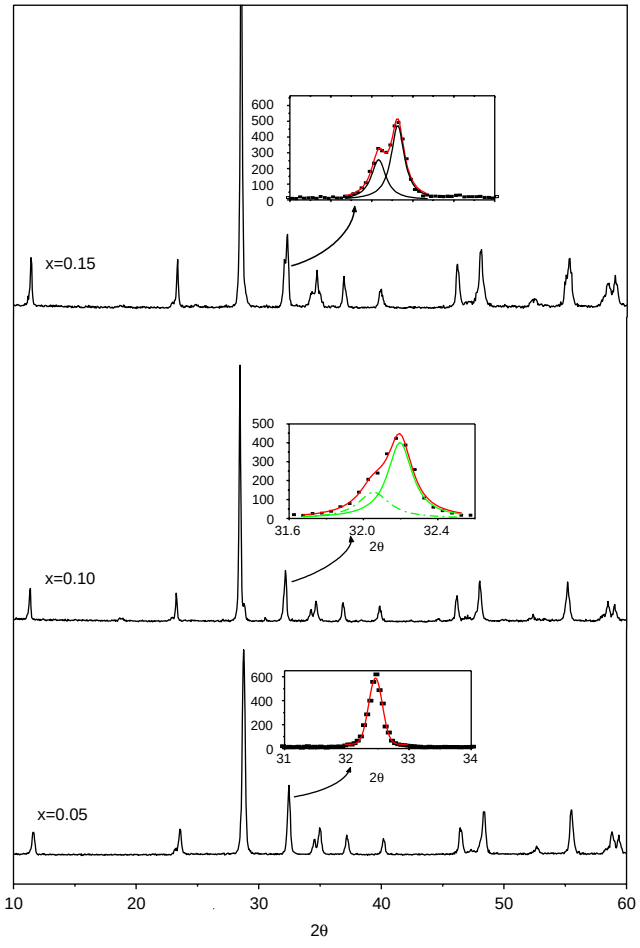

Fig. 1. X-ray diffraction patterns of $Bi_4V_{1.8}Cu_{0.2-x}Nb_xO_{10.7+3x/2}$.

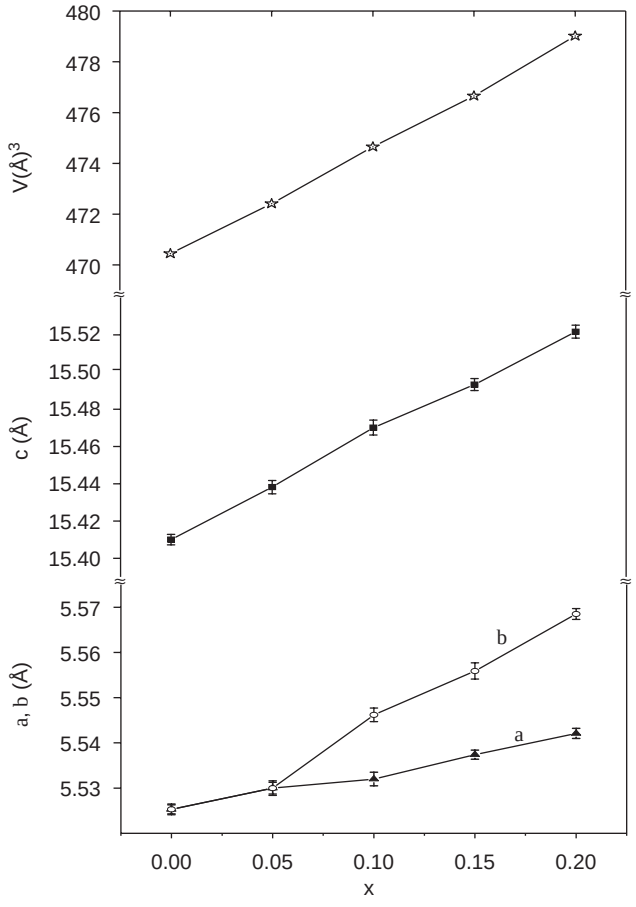

Fig. 2. Evolution with x of the lattice parameters and the cell volume of $Bi_4V_{1.8}Cu_{0.2-x}Nb_xO_{10.7+3x/2}$ solid solution.

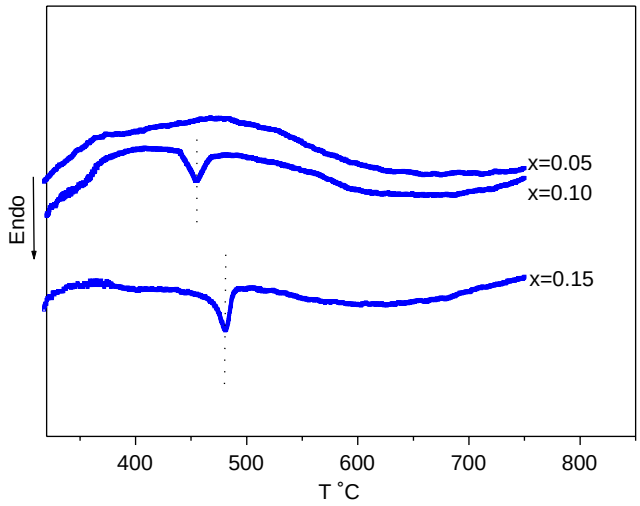

Fig. 3. DTA thermograms for $Bi_4V_{1.8}Cu_{0.2-x}Nb_xO_{10.7+3x/2}$ solid solution.

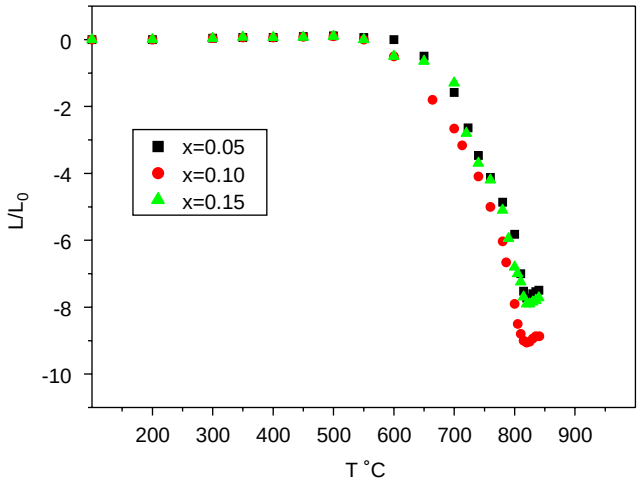

Fig. 4. Temperature dependence of the shrinkage of $Bi_4V_{1.8}Cu_{0.2-x}Nb_xO_{10.7+3x/2}$ solid solution

effective ionic radius of Cu^{2+} and Nb^{5+}, which behaves in the opposite direction. Nevertheless, in our case the volume increase induced by $3x/2$ atoms of oxygen that fill the $3x/2$ vacancies in the anionic sublattice is predominant.

The DTA thermograms recorded for three samples with $x = 0.05$, 0.10 and 0.15 are presented in Fig. 3. As it can be seen, only one endothermic peak was observed on heating for materials with $x = 0.10$ and 0.15, while no thermal effect has been detected for the compound with $x = 0.05$. The peaks observed for the two first materials are assigned to $\beta \rightarrow \gamma$ transition. The $\alpha \rightarrow \beta$ transition appears to be suppressed. The absence of any peak in the trace of the sample with $x = 0.05$ confirms its tetragonal symmetry and is in good agreement with the above X-ray results.

The TG traces (not represented here) show no weight loss in all the studied temperature range.

3.2. Sintering behaviour and characterization of the microstructure

The temperature dependence of the shrinkage for $Bi_4V_{1.8}Cu_{0.2-x}Nb_xO_{10.7+3x/2}$ ceramics is represented in Fig. 4. The shrinkage starts for all compositions at about 600 °C. After this temperature, the three samples exhibit almost the same temperature evolution until 800 °C. At this temperature the shrinkage reaches a value of 7.5% for $x = 0.05$ and 0.15, and 9% for $x = 0.10$. The curves remain practically constant after that temperature till 820 °C. A slight increase of the volume of the disk is then observed after 820 °C.

The influence of sintering time on the ceramics shrinkage has also been studied at two sintering temperatures 800 °C (Fig. 5) and 830 °C (Fig. 6). At 800 °C the shrinkage is almost complete in 10 h while its

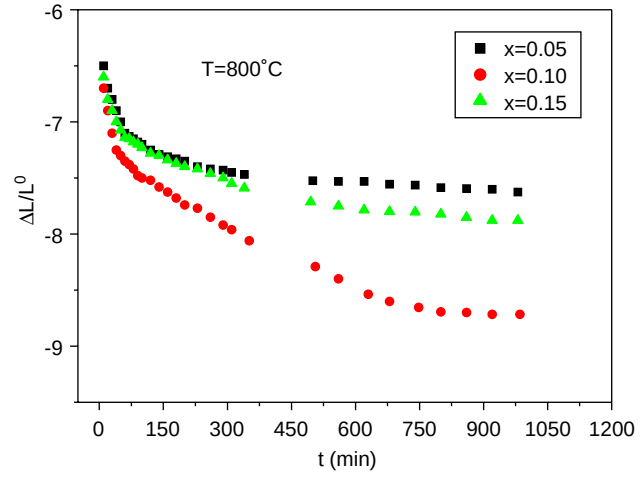

Fig. 5. Influence of sintering time on the shrinkage of ceramics of $Bi_4V_{1.8}Cu_{0.2-x}Nb_xO_{10.7+3x/2}$ solid solution at 800 °C.

ends practically in 1 h at 830 °C. After 2 h we observe here also an increase of the volume of the disk.

A study of the microstructure was carried out with scanning electron microscopy to clarify the origin of the increase of the volume of our materials sintered at temperatures higher than 820 °C. Since the increase of the ceramic shrinkage could be due to the quenching of the samples, the pellets used for the microscopy observations were slowly cooled to room temperature from the sintering temperature. All the compositions were found to have an identical morphology with clearly seen grain boundary. Typical scanning electron micrographs of $Bi_4V_{1.8}Cu_{0.1}Nb_{0.1}O_{10.85}$ sample sintered at two temperatures 800 and 830 °C for 10 h is depicted in Fig. 7. The ceramic sintered at 800 °C shows intermediate grain sizes ≈8–12 μm with a residual porosity, along grain boundaries (Fig. 7a). The grain size increases when increasing the sintering temperature

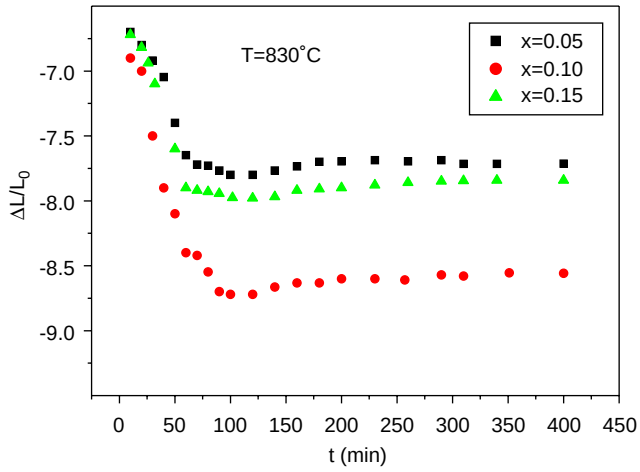

Fig. 6. Influence of sintering time on the shrinkage of ceramics of $Bi_4V_{1.8}Cu_{0.2-x}Nb_xO_{10.7+3x/2}$ solid solution at 830 °C.

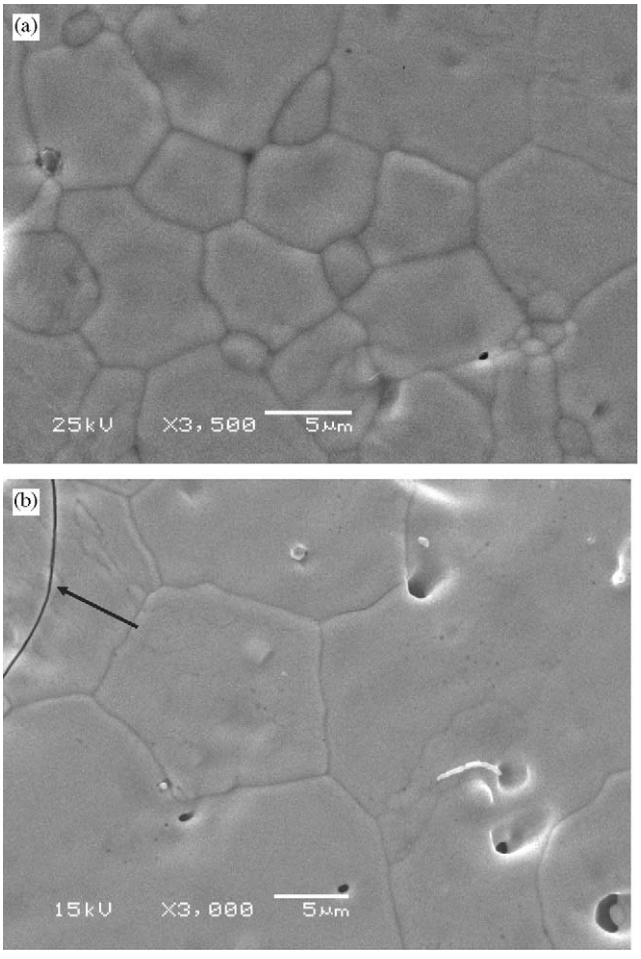

Fig. 7. SEM micrographs of $Bi_4V_{1.9}Cu_{0.1}Nb_{0.1}O_{10.7}$ sintered during 10 h at 800 °C (a) and 830 °C (b). (micro-craks are indicated by arrows).

and is ranging between 15 and 20 μm (Fig. 5b). In addition to the increase of the grain size we observe also micro-cracks (indicated by the arrow). These micro-cracks have been previously observed in other BIMEVOX compounds and have been attributed to the anisotropy of the BIMEVOX materials [27,32,35]. Therefore, the increase of the volume of the pellets seems to be a consequence of the presence of these micro-cracks. This feature concerns not only the substituted phases but also the parent compound $Bi_4V_2O_{11}$, since they appear clearly on the scanning electron micrographs of unetched ceramics sintered at 797 °C for more than 36 h in the Prasad's et al. publication dealing with grain size effect on the dielectric properties of ferroelectric $Bi_4V_2O_{11}$ [36]. The use of conventional synthesis and milling results, in most times, in materials with low density associated to micro-crack. So, alternative chemical synthesis routes such as co-precipitation or sol–gel process, which are expected to reduce the particle size, could suppress this anomalous microstructure.

3.3. Electrical conductivity

To evaluate the reproducibility of the conductivity measurements, two pellets with similar size parameters and weights were used for each composition; and no significant difference was observed between the conductivity values obtained for the two pellets (less than 3%).

Typical Nyquist plots obtained for medium (248 °C) and high temperatures (680 °C) are reported on Fig. 8a. At 248 °C the impedance spectra is characterised by two asymmetric arcs at high frequencies and a straight line at low frequencies. The mean value of the capacitance is about 8×10^{-11} F, which is usually found for bulk response [37]. The second semicircle is assigned to the grain boundary contribution while the straight line is characteristic of the interfacial processes at the blocking electrodes.

For high temperatures, the electrolyte and electrode contributions to the cell impedance were deconvoluted as shown in Fig. 6b. In the limit of high frequency (>15 kHz), the total impedance was typically ohmic or purely inductive, with a real value R_{ohmic}, corresponding to the sample resistance and the connecting wires impedance. The remaining impedance $Z_{interface}$ was taken to be the impedance of the electrodes reactions. When the temperature increases the high frequencies semi-circles disappears and the double layer contribution becomes more visible.

The logarithmic plots of the electrical conductivity as a function of the reciprocal temperature obtained between 140 and 680 °C are shown in Fig. 9. For the materials with $x = 0.10$ and 0.15 only one transition is observed: at about 460 °C for the compound with $x = 0.10$ and at 480 °C for that with $x = 0.15$. This discontinuity is assigned to the $\beta \rightarrow \gamma$ transition. However, the conductivity curve of the compound with $x = 0.05$ is characterized by a curvature around 480 °C, while no thermal effect is observed by DTA analysis.

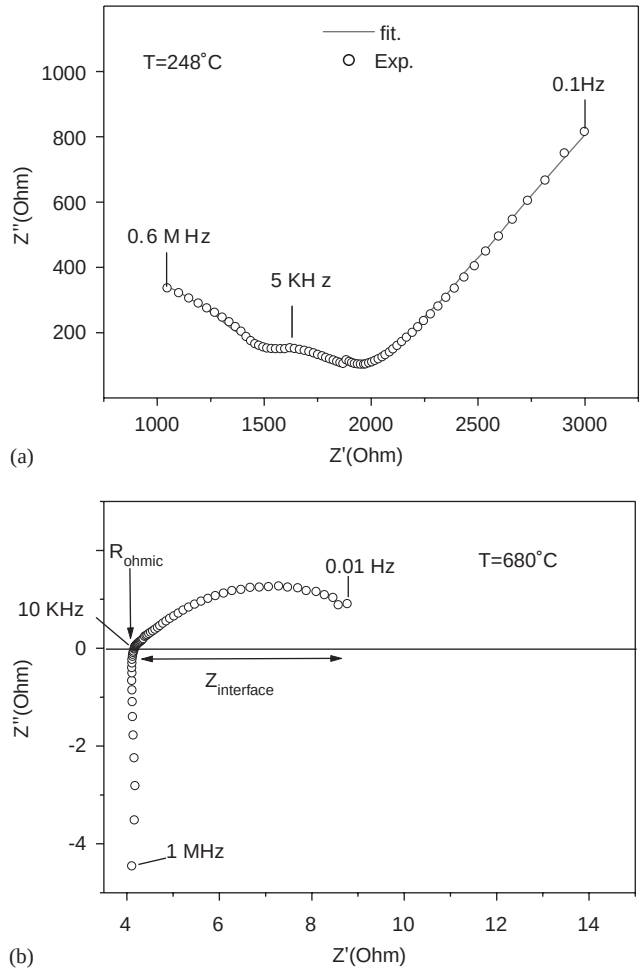

Fig. 8. Nyquist plots for $Bi_4V_{1.8}Cu_{0.1}Nb_{0.1}O_{10.7}$ sample at 248 °C (a) and 680 °C (b).

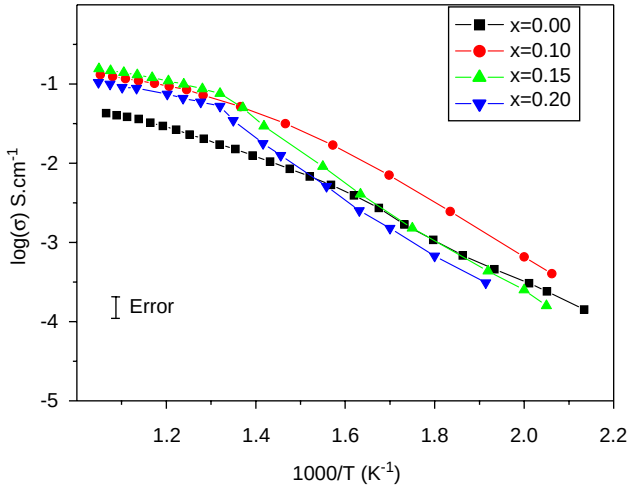

Fig. 9. Temperature dependence of the electrical conductivity of $Bi_4V_{1.8}Cu_{0.2-x}Nb_xO_{10.7+3x/2}$ solid solution.

Therefore, the low temperature form with tetragonal symmetry is not a γ polymorph but a γ' one, characterized by a relatively high activation energy ≈ 0.65 eV instead of 0.20–0.40 eV generally found for γ phases. At high temperatures all the samples present almost the same conductivity values and the activation energies are also similar ≈ 0.21 eV. The conductivity reaches $10^{-1}\,\Omega^{-1}\,cm^{-1}$ at 600 °C for $x = 0.05$. However, at temperatures below 450 °C the effect of dopant concentration is apparent and the compound with $x = 0.05$ (γ' phase) presents the highest conductivity. Moreover, the conductivity performances of this compound ($x = 0.05$) are slightly higher than those observed for $Bi_4V_{1.8}Cu_{0.2}O_{10.7}$ (relative density $\approx 83\%$) but comparable to those found for dense $Bi_4V_{1.8}Cu_{0.2}O_{10.7}$ (relative density $\approx 96\%$) [38]. The same behaviour was also observed for $Bi_4V_2O_{11}$ doubly substituted by Cu^{2+}–Ti^{4+} [31].

4. Conclusions

Doping with Nb^{5+} in the $Bi_4V_{1.8}Cu_{0.2}O_{10.7}$ compound leads to the stabilization of the tetragonal γ' polymorph for $x = 0.05$, while the β polymorph is observed for $x = 0.10$ and 0.15. The ceramics sintered at 830 °C for 10 h present micro-cracks, which can be attributed to the anisotropy of the BIMEVOX compounds. The electrical conductivity has been slightly improved compared with the $Bi_4V_{1.8}Cu_{0.2}O_{10.7}$, compound with similar relative density. However, the highest value of conductivity is observed in the compound with $x = 0.05$ rather than $x = 0.10$ such as previously observed.

Acknowledgments

The authors are grateful to CNRS-France and l'Institut de Chimie de la Matière Condensée de Bordeaux for making to the disposal of our Centre an XPERT MPD Philips diffractmeter.

References

[1] B. Aurivillius, Arkiv. Kemi. 1 (1949) 463.
[2] R.W. Wolfe, R.E. Newnham, Solid State Commun. 7 (1969) 1797.
[3] E.C. Subbarao, J. Am. Ceram. Soc. 45 (1962) 166.
[4] I.H. Ismailzade, V.I. Sterenko, F.A. Mirishli, P.G. Rustamov, Sov. Phys. Cristallogr. 12 (1967) 400.
[5] A. Fouskova, L.E. Cross, J. Appl. Phys. 41 (1970) 2834.
[6] J.F. Dourian, R.E. Newnham, D.K. Smith, Ferroelectrics 3 (1971) 17.
[7] I.H. Ismailzade, J. Ravez, Ferroelectrics 21 (1978) 423.
[8] K.R. Kendall, J.K. Thomas, H.-C. Zur Loye, Solid State Ionics 70/71 (1994) 221.
[9] A. Snedden, S.M. Blake, P. Lighfoot, Solid State Ionics 156 (2003) 439.
[10] A.A. Bush, Yu.N. Venevtsev, Rus. J. Inorg. Chem. 35 (5) (1986) 769.

[11] F. Abraham, M.F. Debreuille-Gresse, G. Mairesse, G. Nowogrocki, Solid State Ionics 28–30 (1988) 529.
[12] F. Abraham, J.C. Boivin, G. Mairesse, G. Nowogrocki, Solid State Ionics 40–41 (1990) 934.
[13] J.B. Goodenough, A. Manthiram, M. Paranthaman, Y.S. Zhen, Mater. Sci. Eng. B 12 (1992) 357.
[14] R. Essalim, B. Tanouti, J.P. Bonnet, J.M. Reau, Mater. Lett. 13 (1992) 386.
[15] V. Sharma, A.K. Shukla, J. Goplakrishnan, Solid State Ionics 58 (1992) 359.
[16] J. Yan, M. Greenblatt, Solid State Ionics 81 (1995) 225.
[17] M. Alga, A. Ammar, M. Wahbi, B. Tanouti, J.C. Grenier, J.M. Reau, J. Alloys Compounds 256 (1997) 234.
[18] Y.L. Yang, L. Qui, A.J. Jacobson, J. Mater. Chem. 7 (6) (1997) 937.
[19] F. Krok, I. Abraham, A. Zadrozna, M. Malys, W. Bogug, J.A.G. Nelstropand, A.J. Bush, Solid State Ionics (1998) 138.
[20] A. Castro, P. Millan, P. Sciau, C. Rouan, G. Galy, Mater. Res. Bull. 34 (5) (1999) 655.
[21] C.K. Lee, G.S. Lim, A.R. West, J. Mater. Chem. 4 (1994) 1441.
[22] O. Joubert, A. Jouanneaux, M. Ganne, M. Tournous, Mater. Res. Bull. (1992) 1235.
[23] A.A. Yaremkenko, V.V. Kharton, E.N. Naumovich, V.V. Samokhval, Solid State Ionics 111 (1998) 227.
[24] A. Watanabe, K. Das, J. Solid State Chem. 163 (2002) 224.
[25] C.J. Watson, A. Coats, D.C. Sinclair, J. Mater. Chem. 7 (10) (1997) 2091.
[26] M. Alga, A. Ammar, R. Essalim, F. Mauvy, R. Decourt, B. Tanouti, Solid State Sciences, submitted for publication.
[27] J.C. Boivin, C. Pirovano, G. Nowogrocki, G. Mairesse, P. Labrune, G. Lagrange, Solid State Ionics 113–115 (1998) 639.
[28] M.E.A. Donpablo, E. Moran, F.G. Alvarado, J. Inorg. Mater. 1 (1999) 83.
[29] G. Mairesse, in: B. Scrosati, A. Magishis, C.M. Mari, G. Mariotto (Eds.), Fast Ion Transport in Solids, Kluwer, Dordrecht, 1993, p. 271.
[30] R.N. Vannier, G. Mairesse, F. Abraham, G. Nowogrocki, Solid State Ionics 70/71 (1994) 248.
[31] M.H. Paydar, A.M. Hadian, G. Fafilek, J. Eur. Ceram. Soc. 21 (2001) 1821.
[32] M. Alga, A. Ammar, R. Essalim, B. Tanouti, F. Mauvy, R. Decourt, Ionics 11 (2005).
[33] O. Joubert, A. Jouanneaux, M. Ganne, R.N. Vannier, G. Mairesse, Solid State Ionics 73 (1994) 309.
[34] R.D. Shanon, Acta Crystallogr. A 32 (1976) 751.
[35] M.C. Steil, J. Fouletier, M. Kleitz, P. Larbure, J. Eur. Ceram. Soc. 19 (1999) 815.
[36] K.V.R. Prasad, A.R. Raju, K.B.R. Varma, J. Mater. Sci. 29 (1994) 2691.
[37] J.R. Mac Donald, Impedance Spectroscopy Emphazing Solid Materials and Systems, Wiley, New York, 1987.
[38] M.H. Paydar, A.M. Hadian, K. Shiamnoe, N. Yamazoe, J. Eur. Ceram. Soc. 21 (2001) 1825.